ANTIOXIDANTS & REDOX SIGNALING
Volume 14, Number 12, 2011

DOI: 10.1089/ars.2010.3574

ORIGINAL RESEARCH COMMUNICATION

Identification of Senescence-Associated Genes and Their Networks Under Oxidative Stress by the Analysis of Bach1

Kazushige Ota,[1,2] Yoshihiro Dohi,[1,3] Andrey Brydun,[1,4] Ayako Nakanome,[1] Sadayoshi Ito,[2,5] and Kazuhiko Igarashi[1,4]

Abstract

Cellular senescence is induced in response to DNA damage, caused by genotoxic stresses, including oxidative stress, and serves as a barrier against malignant transformation. Tumor-suppressor protein p53 induces genes critical for implementing cellular senescence. However, the identities of p53 target genes and other regulators that achieve senescence under oxidative stress remain to be elucidated. Effector genes for oxidative stress–induced cellular senescence were sought, based on the fact that transcription factor Bach1 inhibits this response by impeding the transcriptional activity of p53. pRb became hypophosphorylated more rapidly in *Bach1*-deficient MEFs than in wild-type cells, suggesting that pRb activation was involved in their senescence. *Bach1*-deficient MEFs bypassed the senescence state when the expression of a subset of p53 target genes, including *p21*, *Pai1*, *Noxa*, and *Perp*, was simultaneously reduced by using RNAi. Combined knockdown of p21 and pRb resulted in vigorous re-proliferation. These results suggest that oxidative stress–induced cellular senescence is registered by multiple p53 target genes, which arrest proliferation redundantly, in part by activating pRb. Our elucidations contrast with previous reports describing monopolistic regulations of senescence by single p53 target genes. *Antioxid. Redox Signal.* 14, 2441—2451.

Introduction

Cellular senescence is permanent cell-cycle arrest, which is dependent on the tumor suppressors p53 and pRb (12). Cellular senescence was originally reported by using cultured primary human fibroblasts (20), and it is observed in many types of cells in response to DNA damage caused by oxidative stress, telomere shortening, and oncogenic stress (5, 14). The fact that it can be seen in premalignant tumors (13) shows that it is one of the critical inhibitors of tumor progression. Among the cells in which cellular senescence can be induced, murine embryonic fibroblasts (MEFs) are known to accumulate higher levels of oxidative damage in the presence of higher levels of oxygen (*i.e.*, 20%) and thereby become senescent by the p53-pathway activation (29). Oxidative stress induces DNA damage that can potentially induce genomic instability, which contributes to cancer progression (23, 29). Although the activity of p53 is tightly controlled by several signaling pathways, such as the $p19^{ARF}$-MDM2-p53 pathway (32) and DNA damage repair pathways involving ATM protein kinase (4), it is not clear how p53 activation leads to selection among senescence, transient cell-cycle arrest, and apoptosis (37). Depending on the mechanisms of p53 activation or cellular contexts or both, p53 may activate a subset of its target genes involved in the process of cellular senescence (34). Both *p21* and *Pai1* have been identified as the genes associated with cellular senescence among the known p53 target genes, the former being an inhibitor of cyclin-dependent kinases, and the latter, an inhibitor of the PI(3)K-PKB-GSK3β-cyclinD1-pRb pathway (19, 24). Both p21 and Pai1 indirectly reduce pRb phosphorylation and thereby activate it to promote pRb-dependent senescence. However, cellular senescence cannot be fully explained by them alone. For example, *p21*-deficient MEFs still undergo senescence (28), and a genetic interaction between *p21* and *pRb* has not been examined in the setting of cellular senescence.

Transcription factor Bach1 is a key inhibitor of cellular senescence induced by reactive oxygen species (ROS) (17). Bach1 forms a complex with p53 together with HDAC1 (histone deacetylase 1) and Nco-R (nuclear co-repressor), promotes histone deacetylation by directing HDAC1 to the p53 target genes, and represses their expression at the transcriptional

[1]Department of Biochemistry and [2]Division of Nephrology, Endocrinology, and Vascular Medicine, Tohoku University Graduate School of Medicine, Sendai, Japan.
[3]Department of Cardiovascular Physiology and Medicine, Hiroshima University Graduate School of Biomedical Science, Hiroshima, Japan.
[4]Center for Regulatory Epigenome and Diseases and [5]Center for Advanced and Integrated Renal Science, Tohoku University Graduate School of Medicine, Sendai, Japan.

level to inhibit cellular senescence. *Bach1*-defiecient MEFs enter the senescent state more rapidly than wild-type cells under 20% O_2 conditions because of hyperactivation of p53 (17). In a parallel, p53-independent pathway, Bach1 represses another set of target genes, including heme oxygenase-1 (HO-1), a critical gene for protection against oxidative stress (39). The Bach1 target genes in this category possess a Maf-recognition element (MARE) to which Bach1 binds by forming a heterodimer with the small Maf oncoproteins (22, 27, 39). Thus, Bach1 plays important roles in the regulation of senescence and oxidative-stress response and may integrate these cellular responses.

To clarify the downstream networks of p53 in the process of oxidative stress–induced cellular senescence, *Bach1*-deficient MEFs were used in this study by exploiting their hypersensitivity to oxidative stress (17). We found that no single gene among the known senescence effectors was essential for the maintenance of senescence. A combined knockdown of four genes (*p21, Pai1, Noxa*, and *Perp*) resulted in a weak but reproducible reproliferation, suggesting that multiple p53 subpathways contribute to senescence in a redundant manner. Combinatorial knockdown of *p21* and *pRb* resulted in vigorous reproliferation of senescent cells. Considering the necessity of p21 and pRb for senescence and more rapid reduction in pRb phosphorylation in *Bach1*-deficient MEFs, these observations indicate that the p53–pRb crosstalk was critical for senescence in *Bach1*-deficient MEFs. Our findings suggest that *Bach1* inhibits the process of oxidative stress–induced cellular senescence by modulating expression of the specific downstream subpathways of p53.

Materials and Methods

Isolation and culture of mouse embryonic fibroblasts

MEFs were isolated from 14.5-day-old embryos of various genotypes, as previously described (17). MEFs from single embryos were plated into a 60-mm-diameter culture dish and cultured with DMEM (Gibco, Carlsbad, CA) containing 10% fetal bovine serum (Cell Culture Bioscience, Tokyo, Japan), 1% NEAA (Gibco), 1% penicillin/streptomycin (Gibco), and 4.2 μl 2-mercaptethanol (Wako Junyaku, Osaka, Japan) at 37°C. Cells were cultured in 20% or 3% oxygen by subculturing in a 60- or 100-mm-diameter culture dish every 2 or 3 days, and cell number was determined at each passage. Senescent cells were prepared by several passages for at least 4 weeks (about seven to nine and five to seven passages in wild-type and *Bach1*-deficient MEFs, respectively) under 20% oxygen until they stopped proliferation and showed flattened morphology with SA-β-gal staining. Senescence induced by H_2O_2 was performed by the protocol indicating that confluent fresh MEFs be treated with 550 μ*M* H_2O_2 in serum-containing medium for 2 h, left to recover overnight, as described previously (25), and then used in RNA interference.

RNA interference

Stealth RNAi duplexes were designed for the target genes by using the BLOCK-iT RNAi Designer (Invitrogen Corporation, Carlsbad, CA). For the knockdown of the target genes, 2.0×10^6 cells were transfected with 6 μl of stock Stealth RNAi duplexes (20 μ*M*) by using the basic nucleofection solution for MEFs (VPD-1004; Lonza, Koeln, Germany). Stealth RNAi Negative Control duplexes (Invitrogen Corporation) were used as negative control RNAi. The transfected cells were divided into three parts and cultured in 60-mm-diameter culture dishes. Cell number was determined at the indicated days, and data are reported in figures as relative values compared with cell numbers at day 1. Sequences of the Stealth RNAi used in this study were as follows:

p53 RNAi, 5′-UUACACAUGUACUUGUAGUGGAUGG-3′
cdkn2a RNAi 5′-UUAGCUCUGCUCUUGGGAUUGGCCG-3′
HO-1 RNAi, 5′-AUCACCAGCUUAAAGCCUUCUCUGG-3′
p21 RNAi, 5′-UUGGAGUGAUAGAAAUCUGUCAGGC-3′
Pai1 RNAi, 5′-UUGACUUUGAAUCCCAUAGCAUCUU-3′
Noxa RNAi, 5′-AUACCAGGCAUUUCCAUCAACCGGC-3′
Perp RNAi, 5′-UUAUCGUGAAGCCUGAAGGUCUGUG-3′
Notch1 RNAi, 5′-ACGCCGCUGUGAGUCAGUCAUCAAU-3′
Lrdd RNAi, 5′-AGAACUUCUCACCCUCAAACAUCUC-3′
Gpx1 RNAi, 5′-ACUUGAGGGAAUUCAGAAUCUCUUC-3′
Fat1 RNAi, 5′-AAAUGAUGUGAACAACUUUCACGGG-3′
Bcas3 RNAi, 5′-AGAACUAGUUGAUAUGACCGUGGUC-3′
Pcdh7 RNAi, 5′-UGUACAGGCUCAUCUCUGCAUUCCG-3′
Prl-3 RNAi, 5′-CUUUGAACCUCAGUCUCUGCUUAGG-3′
Rb1 RNAi, 5′-UUUAGUCGGAGAUAUGCUAGACGGU-3′

Senescence-associated β-galactosidase staining and cell-cycle analysis

MEFs were stained overnight for senescence-associated (SA) β-galactosidase, as previously reported (15). Incubated for 16 h with 10 μ*M* BrdU with BrdU Flow Kits (BD Pharmingen, San Jose, CA), cytometric analyses of MEFs were performed on a FACSCalibur with CellQuest software (Becton Dickinson, Franklin Lakes, NJ).

Expression profiling, RNA amplification, and Q-PCR

Preparation of total RNAs from various cells was carried out by using the Total RNA Isolation minikit (Agilent Technologies, Palo Alto, CA). Agilent whole-mouse genome (4x44K, G4122F) arrays were used for this study, as described previously (17). The analysis and clustering of genes were performed by using the Genespring software package (Agilent Technologies). The quantitative PCRs were performed with a LightCycler (Roche). Primers used were as follows:

p53, (forward) 5′-GGAGGAGTCACAGTCGGAT-3′
(reverse) 5′-GCTTCACTTGGGCCTTCA-3′
p16, (forward) 5′-TGCGGGCACTGCTGGAAG-3′
(reverse) 5′-GGTAGTGGGGTCCTCGCAGTT-3′
$p19^{ARF}$, (forward) 5′-GCTCTGGCTTTCGTGAACA-3′
(reverse) 5′-TCGAATCTGCACCGTAGTTG-3′
p21, (forward) 5′-CCTGGTGATGTCCGACCTGTT-3′
(reverse) 5′-GGGGAATCTTCAGGCCGCTC-3′
Pai1, (forward) 5′-TTAGTGCAACCCTGGCCGAC-3′
(reverse) 5′-TGCGGGCTGAGATGACAAA G-3′
Noxa, (forward) 5′-GTGCACCGGACATAACTG-3′
(reverse) 5′-AGCACACTCGTCCTTCAAG-3′
Perp, (forward) 5′-GCTGCAGTCTAGCAACCACA-3′
(reverse) 5′-GAAGCAGATGCACAGGATGA-3′
Prl-3, (forward) 5′-TGCTGAAGGCCAAGTTCTAC-3′
(reverse) 5′-TGAGCTGCTTGCTGTTGA-3′
HO-1, (forward) 5′-GGGTGACAGAAGAGGCTAAG-3′
(reverse) 5′-GTGTCTGGGATGAGCTAGTG-3′

Immunoblotting analysis

The immunoblotting analysis used antibodies against pRb (554136; BD Pharmingen), HO-1 (a kind gift from Prof. Shigeru Taketani, Kyoto Institute of Technology), α-tubulin (B7; Santa Cruz), ppRb (phospho-Rb Ser780) (C84F6, CST), c-*myc* (N262; Santa Cruz). Whole-cell extracts and SDS-PAGE were performed as described previously (17).

Statistical analysis

Data are presented as mean ± SD. All the statistical analyses were done by Student's *t* test or Welch's correction. A value of $p < 0.05$ was considered indicative of significance in all tests.

Results

p53-dependent cellular senescence of Bach1-deficient cells involves precocious pRb hypophosphorylation

Senescent wild-type MEFs are known to bypass senescence on the knockdown of p53 (16). We developed a similar assay by using *Bach1*-deficient MEFs to examine whether p53 was also indispensable for the maintenance of cellular senescence in *Bach1*-deficient MEFs. The knockdown of p53 in senescent *Bach1*-deficient MEFs resulted in resumption of proliferation (Fig. 1A). Similar results were obtained in wild-type cells. Thus, senescence of *Bach1*-deficient MEFs was dependent on continuous p53 activity. The effect of knockdown was confirmed by RT-PCR (Fig. 1B).

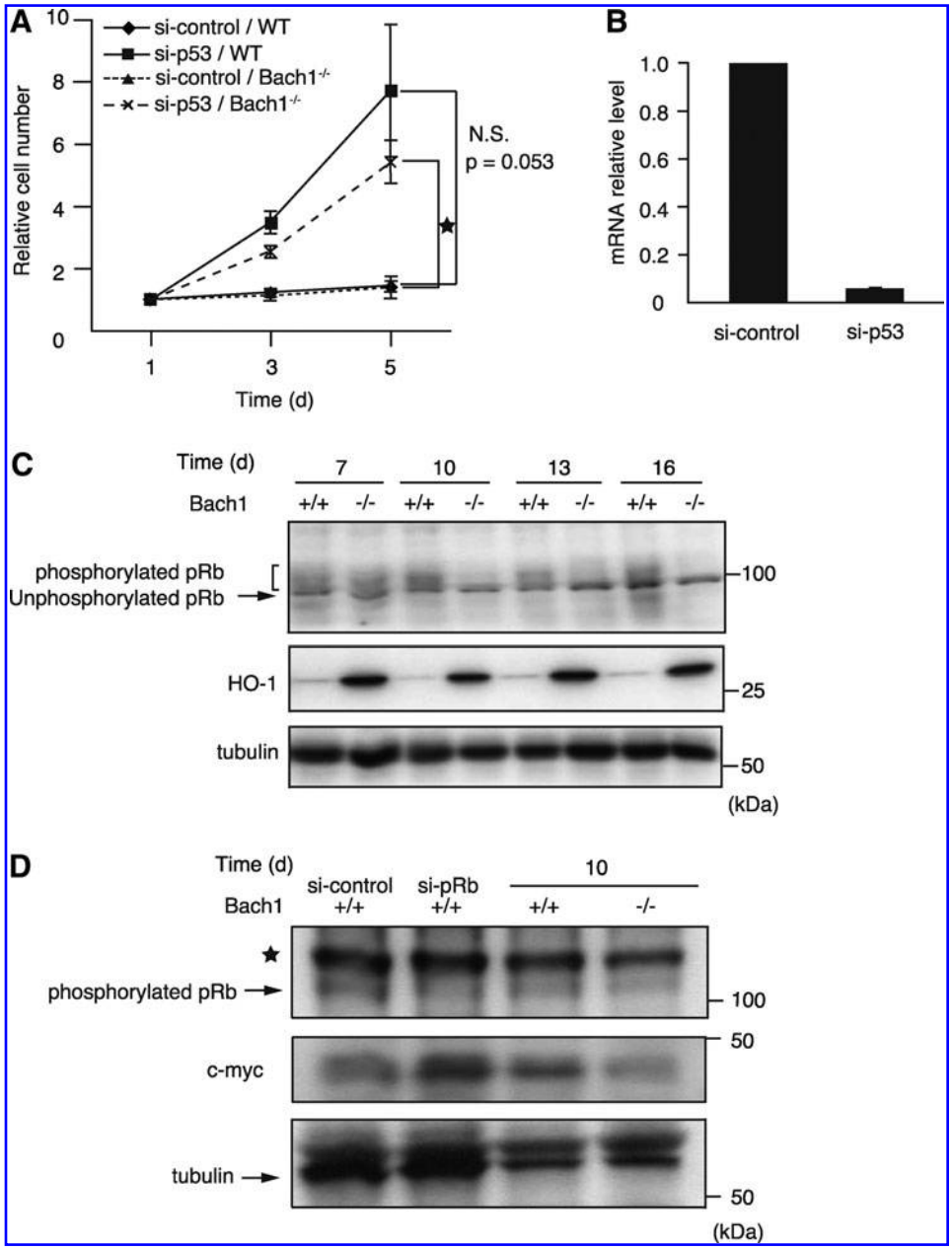

FIG. 1. Analysis of the tumor suppressors p53 and pRb. (A) Proliferation of senescent wild-type and *Bach1*-deficient MEFs expressing RNAi duplexes of control (control RNAi) or *p53* is shown as values relative to day 1. The experiments were performed independently 3 times, and the results are expressed as mean ± SD. *$p < 0.05$. **(B)** *p53* mRNA levels 2 days after RNAi values were determined by qRT-PCR and shown as relative mean values ± SD compared with control RNAi. **(C)** Immunoblotting of pRb, HO-1, and tubulin at the indicated time points (day). The positions of the molecular markers are shown at the right. Phosphorylated pRb forms are indicated with a bracket. The experiments were performed independently 4 times. **(D)** Immunoblotting of phosphorylated pRb, c-*Myc,* and tubulin. Wild-type cells were transfected with control or pRb siRNAs (left two lanes). Wild-type or *Bach1*-deficient cells were cultured for 10 days (right two lanes). The positions of the molecular markers are shown at the right. Specific and nonspecific bands are indicated with *arrow* and *asterisk*, respectively. The experiments were performed independently 4 times.

p53 activates indirectly the pRb tumor suppressor to inhibit the G_1/S transition of the cell cycle, contributing to cellular senescence (8, 40). Considering the crosstalk between p53 and pRb, we examined whether pRb phosphorylation in *Bach1*-deficient MEFs was different from that in wild-type MEFs in the process of senescence. The levels of phosphorylated pRb and unphosphorylated pRb were compared between *Bach1*-deficient and wild-type MEFs during passages *in vitro* (Fig. 1C). Although the majority of pRb at day 7 (passage 3) was phosphorylated and migrated slower than the hypophosphorylated form in SDS-PAGE, irrespective of the genotypes, phosphorylated pRb disappeared earlier in *Bach1*-deficient MEFs than in wild-type MEFs on culture *in vitro*. To confirm these observations, antibody against pRb phosphorylated at Ser780 was used. The level of phosphorylated pRb was reduced on knockdown of pRb, verifying the specificity of the antibody. It was lower in *Bach1*-deficient cells than in wild-type cells at day 10 (Fig. 1D). Expression of c-*Myc*, one of the transcriptional targets of E2F, was increased on pRb knockdown in wild-type cells (Fig. 1D). In contrast, c-*Myc* expression was reduced in *Bach1*-deficient MEFs, indicating that the Rb pathway was more activated in *Bach1*-deficient MEFs than in wild-type MEFs (Fig. 1D). Taken together, these results suggest that the early accelerated pRb hypophosphorylation, presumably due to p53 activation, was involved in the rapid senescence entry of *Bach1*-deficient MEFs.

Both p16 and $p19^{ARF}$ are critical for the activation of pRb and p53, respectively (8). To examine whether cellular senescence in *Bach1*-deficient MEFs is dependent on p16/$p19^{ARF}$, simultaneous knockdown of p16 and $p19^{ARF}$ by using siRNA targeting their gene *Cdkn2a* was performed in near-senescent MEFs (Fig. 2A and B). On knockdown, vigorous reproliferation was observed not only in wild-type but also in *Bach1*-deficient MEFs. Besides the tumor-suppressor genes mentioned earlier, HO-1 has been implicated in the regulation of cell proliferation among known *Bach1* target genes. Carbon monoxide, one of the reaction products of HO-1, inhibits cell proliferation by regulating p21 and pRb (31). Consistent with the fact that HO-1 expression is repressed by *Bach1* (22, 39), the expression of HO-1 was much higher in *Bach1*-deficient MEFs than in control cells (Fig. 1C). These previous reports and our present results suggested the possibility that the upregulation of HO-1 might be involved in the maintenance of cellular senescence in *Bach1*-deficient MEFs. However, knockdown of HO-1 in senescent *Bach1*-deficient MEFs did not affect cell proliferation (Fig. 2C). The effect of knockdown was confirmed by RT-PCR (Fig. 2D). These results suggest that HO-1 is not causally associated with the rapid cellular senescence in *Bach1*-deficient MEFs. Taken together, these results suggested that cellular senescence in *Bach1*-deficient MEFs was specifically dependent on p53, pRb, and their upstream regulators p16 and $p19^{ARF}$.

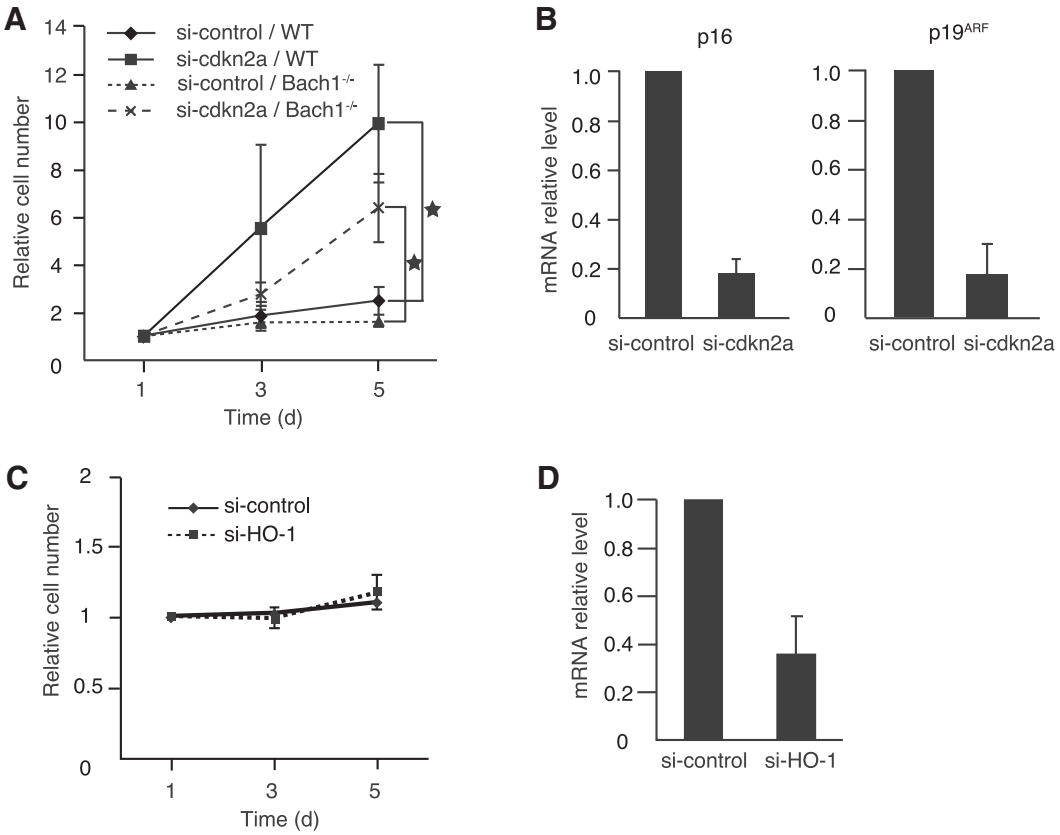

FIG. 2. Oxidative stress–induced cellular senescence involves p16 and 19^{ARF} tumor suppressors but not HO-1. (A) Proliferation of senescent wild-type and *Bach1*-deficient MEFs expressing RNAi duplexes of control (control RNAi) or *Cdkn2a* is shown. **(B)** p16 and $p19^{ARF}$ mRNA levels 2 days after RNAi values were determined by qRT-PCR. **(C)** Proliferation of senescent *Bach1*-deficient MEFs expressing RNAi duplexes of control (control RNAi) or *HO-1*. **(D)** *HO-1* mRNA levels 2 days after RNAi values were determined by qRT-PCR.

Function of Bach1- and p53-co-regulated genes in cellular senescence

The premature senescence of *Bach1*-deficient MEFs is most likely due to de-repression of the p53 target genes because of the absence of Bach1. In search of the putative responsible genes, we focused on a cohort of p53 target genes that were repressed by Bach1. The messenger RNA-expression profiles of two sample sets were compared previously; wild-type and *Bach1*-deficient MEFs (17) and control RNAi and transient Bach1 RNAi in wild-type MEFs. Cells were cultured under conditions of 3% or 20% O_2 to sort genes specifically associated with oxidative stress–induced cellular senescence (17). These profiles identified the genes whose expression was under the control of p53, repressed by Bach1, and induced more under 20% oxygen in comparison to 3% oxygen. In

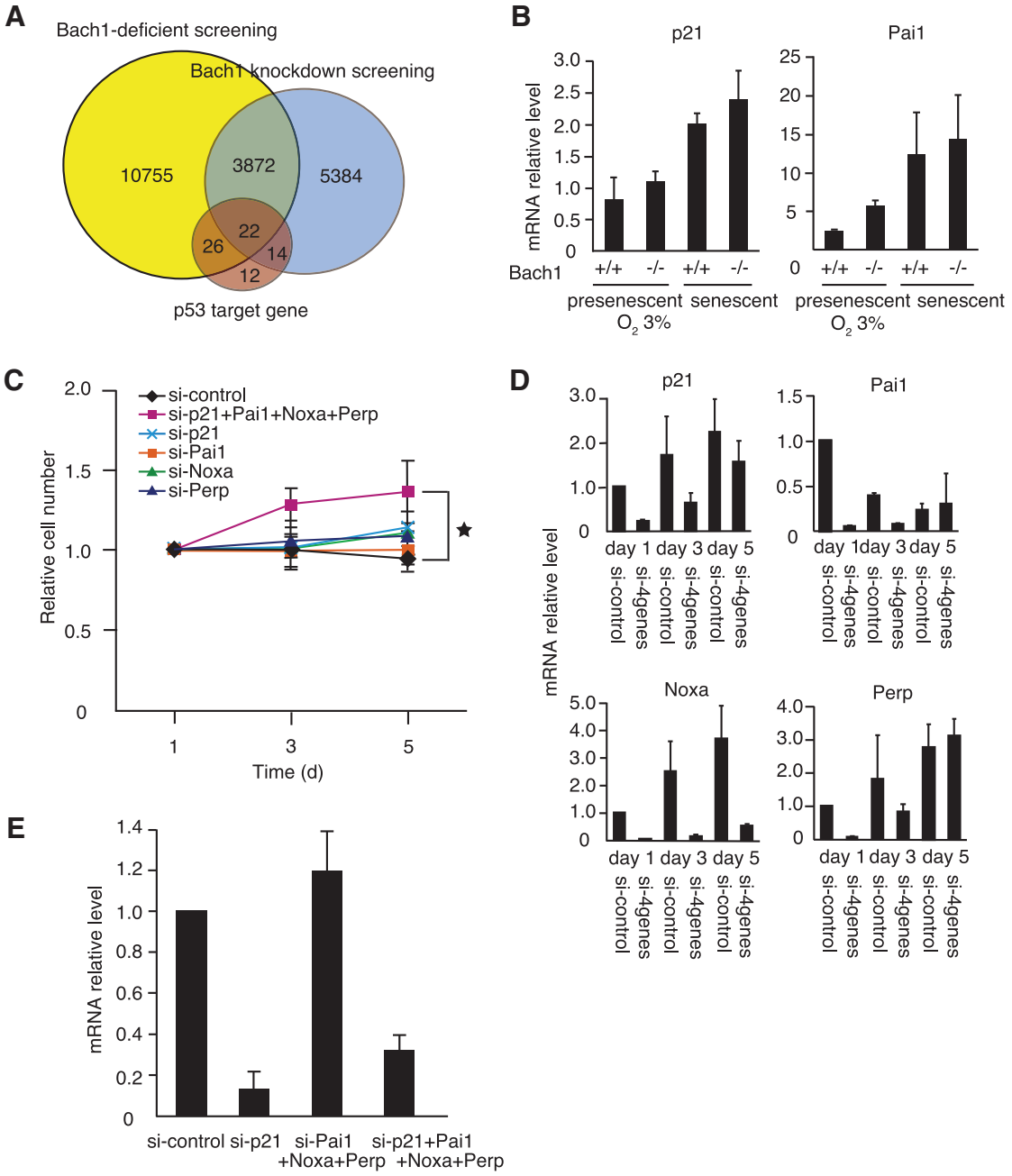

FIG. 3. Detection of senescence-associated genes by means of senescent *Bach1*-deficient MEFs. (A) Venn diagram representation of candidate gene (probe number) screening based on genetic ablation of Bach1 and known p53 direct target gene set. **(B)** Expression of indicated genes in vigorously proliferating (3% oxygen) or senescent cells in wild-type and *Bach1*-deficient MEFs. *p21* and *Pai1* mRNA levels were determined by qRT-PCR. **(C)** Proliferation of senescent *Bach1*-deficient MEFs expressing RNAi duplexes of control (control RNAi) or indicated genes is shown as in Fig. 1A. **(D)** mRNA levels of indicated genes at days 1, 3, and 5 after combinatory RNAi values of p21, Noxa, Pai1, and Perp were determined by qRT-PCR. **(E)** p21 mRNA levels after RNAi of p21, or the combinatorial knockdown were determined by qRT-PCR.

addition, acute knockdown of Bach1 in wild-type MEFs was performed to sort out genes that were indirectly affected by Bach1 knockout (Fig. 3A). Representative genes were selected for further studies from those that are known to regulate apoptosis, cell-cycle arrest (including pRb regulation), or ROS metabolism (Table 1). Among the candidate genes, levels of p21 and Pai1 mRNA, for example, were low in cells cultured under the 3% oxygen condition, which suppressed oxidative stress and senescence, irrespective of the genotype. Conversely, their expression increased when cells became senescent (Fig. 3B). We reported previously that expression of p21 and Pai1 mRNA was higher in *Bach1*-deficient, presenescent MEFs than in wild-type presenescent cells exposed to oxidative stress under 20% oxygen condition (17). Therefore, these observations also fortified the idea that cellular senescence in *Bach1*-deficient MEFs was rapidly induced, but its molecular mechanism seemed to be similar to that of wild-type MEFs.

The expression of these genes was then reduced in senescent *Bach1*-deficient MEFs to examine whether their increased expression in *Bach1*-deficient MEFs was causative of senescence. The cell proliferation, cell morphology, and SA-β-galactosidase activity staining did not change with the individual knockdown of *p21*, *Pai1*, *Noxa*, *Perp*, or the seven other genes (Fig. 3C and data not shown). To explore the possibility that several genes worked redundantly to maintain senescence, four genes were inhibited simultaneously in various combinations. A combinatorial knockdown of *p21*, *Pai1*, *Noxa*, and *Perp* showed a weak but reproducible tendency to bypass cellular senescence in senescent *Bach1*-deficient MEFs (Fig. 3C). RT-PCR at days 1, 3, and 5 revealed that simultaneous knockdown of these genes lasted for at least 3 days after transfection (Fig. 3D). To verify that the knockdown of one gene would not affect the expression of other genes, p21 mRNA levels were compared between combined knockdown with or without *p21* (Fig. 3E). The results indicated that the combinatorial knockdown of *Noxa*, *Pai1*, and *Perp* did not affect p21 mRNA levels. Therefore, the effect of combinatorial knockdown could not be explained by an additional reduction of their mRNA levels by targeting others.

Examinations of cell morphology and SA-β-galactosidase activity confirmed that the combined knockdown of the four genes bypassed cellular senescence in senescent *Bach1*-deficient MEFs (Fig. 4A and B). Changes in cell morphology and expression of SA-β-galactosidase activity are independent of cell-cycle arrest but often are associated with senescence. Although senescent MEFs showed enlarged and flattened morphology, more cells showed sharper and smaller cytoplasmic regions on knockdown of the four genes, similar to p53 knockdown. Cell-cycle analysis by BrdU labeling also validated clearly that the cells resumed S-phase entry on the combined knockdown of these genes (Fig. 4C). Simultaneous knockdown of the four genes also resulted in a tendency to reproliferate in wild-type MEFs, although the effect was not statistically significant (Fig. 4D). These results suggested that the functions of the four genes were not specific to cellular senescence in *Bach1*-deficient MEFs. However, the effect obtained by the combined knockdown was not as profound as the knockdown of p53 in these cells. In contrast to the combination of *p21*, *Pai1*, *Noxa*, and *Perp*, other combinations did not show apparent effect on senescence, including genes such as *Notch1*, leucine-rich and death-domain containing (*Lrdd*), glutathione peroxidase1 (*Gpx1*), FAT tumor-suppressor homolog 1 (*Fat1*), protocadherin7 (*Pcdh7*), and breast carcinoma amplified sequence3 (*Bcas3*) (Fig. 5A). These genes are involved in development, proliferation, apoptosis, oxidative stress, migration, tumor suppression, and adhesion (2, 9, 10, 21, 33, 38). We also carried out knockdown of phosphatase of regenerating liver-3 (*Prl-3*), which has recently been reported to induce G_1 arrest downstream of p53 (6). Whereas the expression of *Prl-3* was higher in *Bach1*-deficient MEFs than in wild-type MEFs, its expression was not affected by the acute knockdown of Bach1 (data not shown). The knockdown of *Prl-3* did not result in bypassing cellular senescence (Fig. 5B). The efficient knockdown of *Prl-3* or other genes was confirmed by RT-PCR (Fig.

Table 1. Candidates for Senescence-associated Genes

GB accession number	*Common name*	*Product*
NM_007387 AK077006	Acp-2	Acid phosphatase 2, lysosomal
NM_007570	Btg2; TIS20	B-cell translocation gene 2, antiproliferative
NM_029791		Bicaudal D homologue 2 isoform 2
NM_138681	rudhira	Breast carcinoma amplified sequence 3-like
NM_007669	P21	Cyclin-dependent kinase inhibitor 1A (P21)
U23536	Fath; mFat1	Cadherin-related cell-adhesion molecule
NM_008160	CGPx; GPx-1	Glutathione peroxidase 1
NM_019919	Tgfb; Ltbp-1	Latent transforming growth factor β-binding protein 1 isoform LTPB-1L
NM_022654	Pidd	Leucine-rich and death domain containing
NM_010179		Mus musculus fat tumor suppressor homolog (Drosophila) (Fath), mRNA
NM_008714	Mis6; Tan1	Notch gene homolog 1 (Drosophila)
Z11886	Mis6; Tan1	Notch gene homologue 1 (*Drosophila*)
NM_022032	PERP	p53 apoptosis effector related to Pmp22
NM_021451	Noxa	Phorbol-12-myristate-13-acetate–induced protein 1
NM_026221		PTPRF-interacting protein, binding protein 1 (liprin beta 1)
NM_008871	PAI1	Serine (or cysteine) proteinase inhibitor, clade E, member 1
NM_013671	MnSOD	Superoxide dismutase 2, mitochondrial
NM_010786	Mdm-2	Transformed mouse 3T3 cell double minute 2

A list of p53 target genes that were upregulated in *Bach1*-deficient MEFs in comparison with wild-type MEFs and in acute knockdown in comparison with control RNAi in wild-type MEFs under 20% O_2. The same GB accession number genes are not shown.

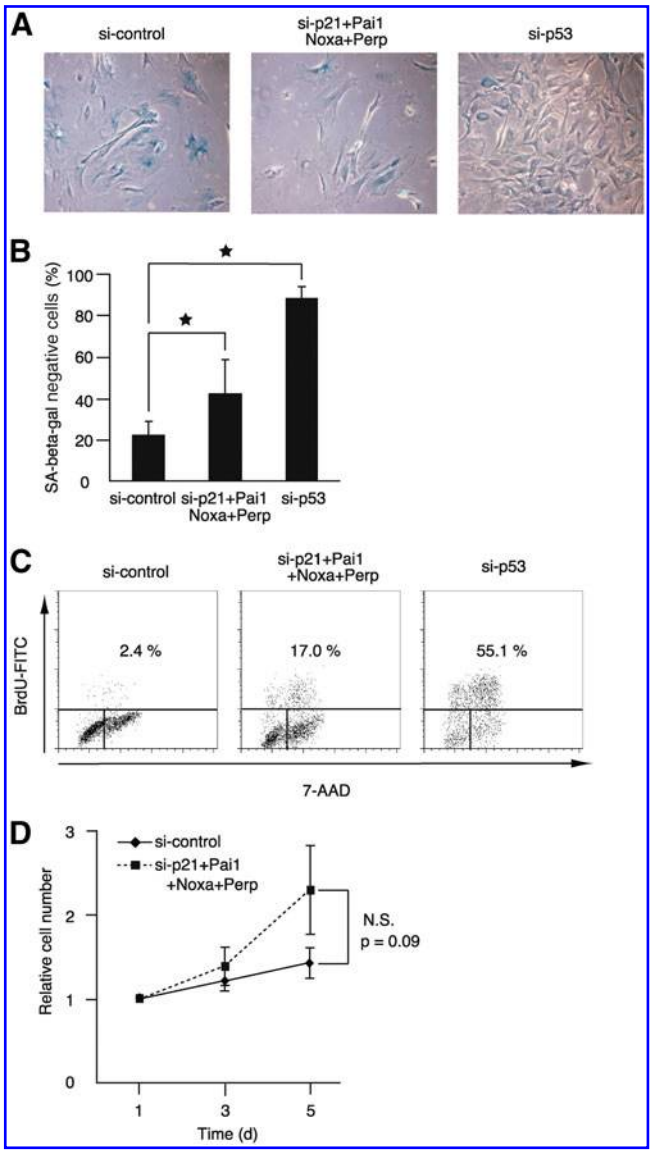

FIG. 4. Involvement of p53 target genes set in cellular senescence. (A, B) Senescence-associated β-galactosidase activity staining 5 days after knockdown of *p21*, *Noxa*, *Pai1*, and *Perp* is shown as representative pictures **(A)**, and the percentages of negative cells as mean ± SD $*p < 0.05$ **(B)**. The experiments were performed independently 5 times. **(C)** A cell-cycle analysis of *Bach1*-deficient MEFs 3 days after knockdown of indicated genes, as in **(B)**. Representative is shown from three independent experiments. **(D)** Proliferation of senescent wild-type MEFs expressing RNAi duplexes of control or the four genes set is shown as in Fig. 1A.

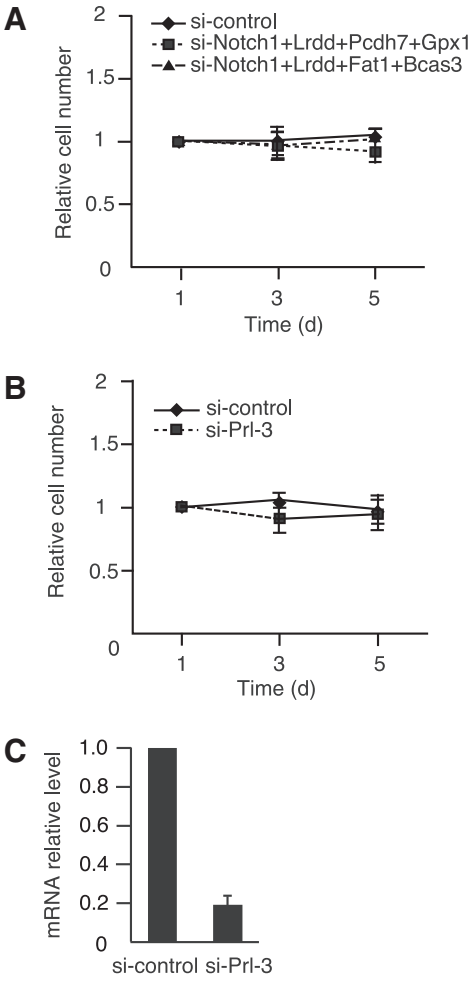

FIG. 5. Specificities of p53 target genes in the regulation of cellular senescence. (A, B) Proliferation of senescent *Bach1*-deficient MEFs expressing RNAi duplexes of control or indicated genes is shown as in Fig. 1A. **(C)** *Prl-3* mRNA levels 2 days after RNAi values were determined by qRT-PCR and shown as in Fig. 1B.

5C and data not shown). Taken together, these results suggest that a distinct subset of p53 target genes, including *p21*, *Pai1*, *Noxa*, and *Perp*, plays important roles in the execution of cellular senescence in response to oxidative stress.

Involvement of p21-pRb subpathway in cellular senescence

Because pRb hyperphosphorylation disappeared more rapidly in *Bach1*-deficient MEFs (Fig. 1C), we examined whether cellular senescence in *Bach1*-deficient MEFs was dependent on pRb. Acute knockdown of *pRb* in senescent *Bach1*-deficient MEFs resulted in weak but reproducible resumption of proliferation (Fig. 6A), consistent with a previous report of using an acute, inducible knockout of *pRb* in senescent wild-type MEFs (35). Efficient knockdown of *pRb* was confirmed by immunoblotting (Fig. 6B). The result that the bypassing effect was not so robust as p53 knockdown suggests that pRb constitutes a pathway redundant with some of the p53 subpathways for senescence. To address this assumption, we tested for a genetic interaction of *pRb* with the four critical p53 target genes. Combinatorial knockdown of *pRb* with *p21*, *Pai1*, *Noxa*, and *Perp* resulted in a more-efficient bypass of senescence than the individual knockdown of *pRb* or the p53 target genes subset (Fig. 6A; see Fig. 3). However, the combinatorial knockdown of *p21*, *Pai1*, *Noxa*, and *Perp* did not affect pRb phosphorylation (Fig. 6C). Because reproliferating cells were the minor fraction of the cells (see Fig. 4C), the effect on pRb, if any, may be masked at the population level. Similar effects in cell proliferation were observed in senescent wild-type MEFs (data not

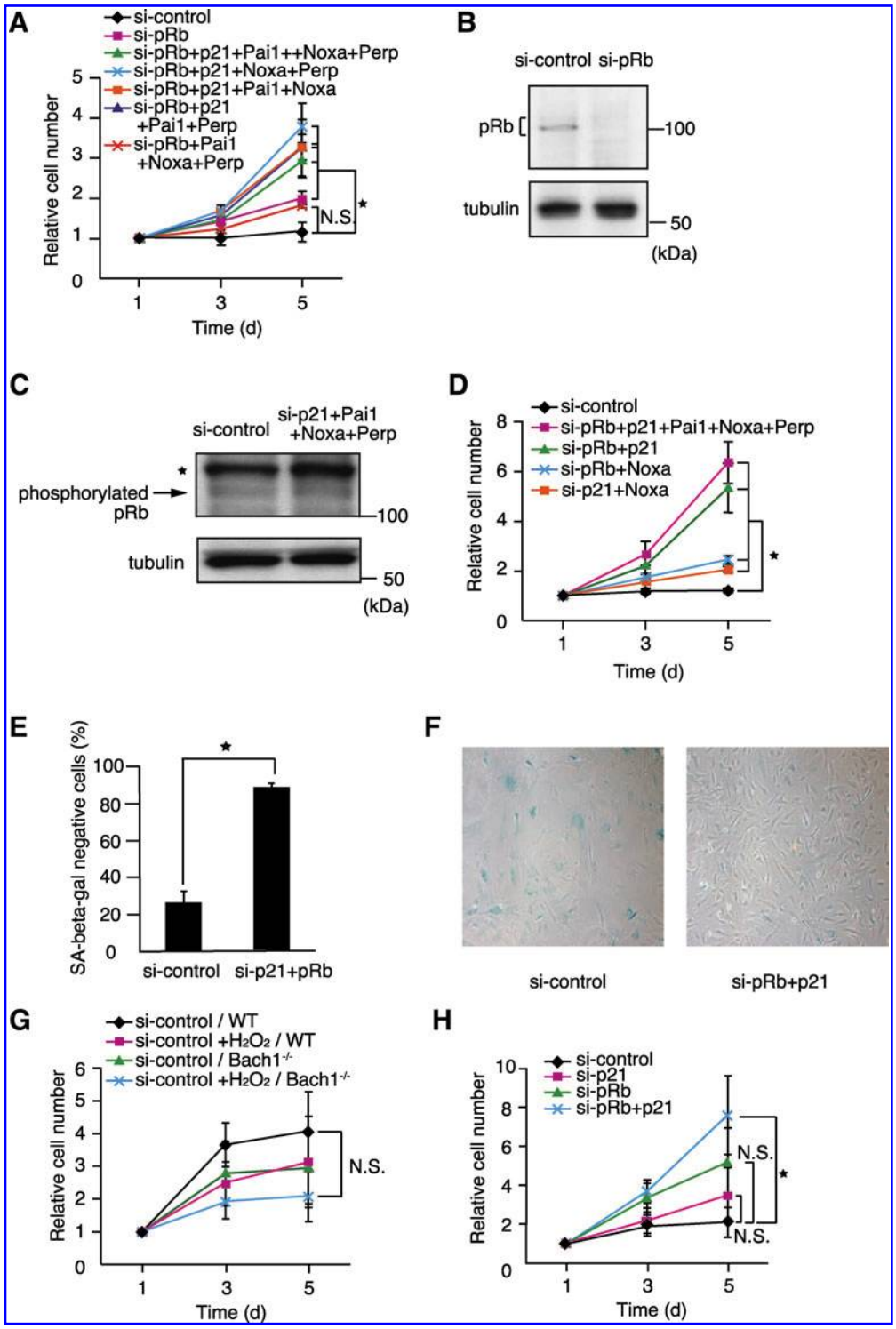

FIG. 6. Cross-talk of p53 target genes subsets and pRb. (A, D) Proliferation of senescent *Bach1*-deficient MEFs expressing Stealth RNAi duplexes of control or indicated combinations of genes is shown as in Fig. 1A. **(B)** The effect of RNAi on pRb protein. The positions of the molecular markers are shown at the right. Representative is shown from two independent experiments. **(C)** Immunoblotting of phosphorylated pRb and tubulin. Proteins were harvested 1 day after the knockdown of control or the indicated combination in presenescent *Bach1*-deficient MEFs. The positions of the molecular markers are shown at the right. Phosphorylated pRb and nonspecific bands are indicated with *arrow* and *asterisk*, respectively. The experiments were performed independently 3 times. **(E, F)** Senescence-associated β-galactosidase activity staining 5 days after knockdown of *p21* and pRb. Percentages of negative cells as mean ± SD **(E)** and representative pictures **(F)** are shown. $*p < 0.05$. **(G)** Proliferation of presenescent wild-type and *Bach1*-deficient MEFs treated with or without hydrogen peroxide. **(H)** Proliferation of presenescent *Bach1*-deficient MEFs treated with hydrogen peroxide and transfected with Stealth RNAi duplexes of control or indicated combinations of genes.

shown), indicating that their genetic interaction was not specific to *Bach1*-deficient MEFs.

To identify critical p53 target gene(s) that collaborate with *pRb*, the combinatorial knockdown of *pRb* with three of the four genes was performed (Fig. 6A). All of the effective combinations included *p21*. The critical functions of *p21* and *pRb* were confirmed by the observation that knockdown of *p21* and *pRb* bypassed senescence as efficiently as the combination of *pRb* with the four p53 target genes (Fig. 6D). The cell morphology and SA-β-galactosidase activity staining confirmed that knockdown of *p21* and *pRb* bypassed cellular senescence (Fig. 6E, F). In contrast, the knockdown of *pRb* and *Noxa* or other p53 target genes did not show any enhancement of bypassing cellular senescence (Fig. 6D and data not shown).

The involvement of p21 and pRb was further examined in the induction of senescence in response to hydrogen peroxide, another oxidative stress agent that is widely used to induce senescence acutely (25). In response to hydrogen peroxide, both presenescent wild-type and *Bach1*-deficient MEFs stopped proliferation (Fig. 6G). The simultaneous knockdown of *p21* and *pRb* in presenescent *Bach1*-deficient MEFs resulted in restoration of vigorous proliferation in comparison to the single knockdown of either gene (Fig. 6H). Taken together, these observations indicated that both *p21* and *pRb* were necessary simultaneously for the induction and maintenance of cellular senescence in response to oxidative stress.

Discussion

This study focused on the altered gene-expression profiles of *Bach1*-deficient MEFs to identify genes and their genetic interaction implementing cellular senescence in response to oxidative stress. Among the candidate genes, the knockdown experiments using senescent *Bach1*-deficient MEFs showed that multiple p53 target genes, including *p21*, *Noxa*, *Pai1*, and *Perp*, functioned redundantly to maintain cellular senescence. Importantly, the observed genetic interaction of *p21* and *pRb* in cellular senescence is the first report and is reminiscent of the accelerated proliferation in *p21/pRb*-double deficient MEFs (11). The additive effect of *p21* and *pRb* knockdown is explained by the canonic p21-pRb pathway (7) and implied that they constituted parallel, redundant pathways as well. This may involve other functions of p21, such as the activation of Rb family p107 and p130, which are also involved in senescence (36) or the inhibition of PCNA required for DNA synthesis (1). In contrast to *p21*, the other three genes (*Pai1*, *Noxa*, and *Perp*) can be placed within the pRb pathway because their combined knockdown did not show any additive effect. Although Pai1 is known to play an important role in pRb activation, Noxa and Perp have not been implicated in senescence thus far (3, 26), leaving their molecular functions unclear. Because combined knockdown of *p21*, *Noxa*, *Pai1*, and *Perp* was not as effective as that of *p21* and *pRb* or *p53*, we surmise that an additional p53 target gene(s) is involved in the pRb-pathway activation (gene X in Fig. 7). Taken together, these observations suggest that p53 achieves cellular senescence by combined action of several, redundant genes affecting the pRb-dependent or -independent subpathways (Fig. 7). The critical role of Bach1 in regulating p53 target genes suggests that Bach1 may be involved in the process of tumorigenesis. We have found that Ras^{V12}-mediated transformation of immortalized MEFs requires Bach1 *in vitro* (A. Nakanome *et al.*, unpublished data).

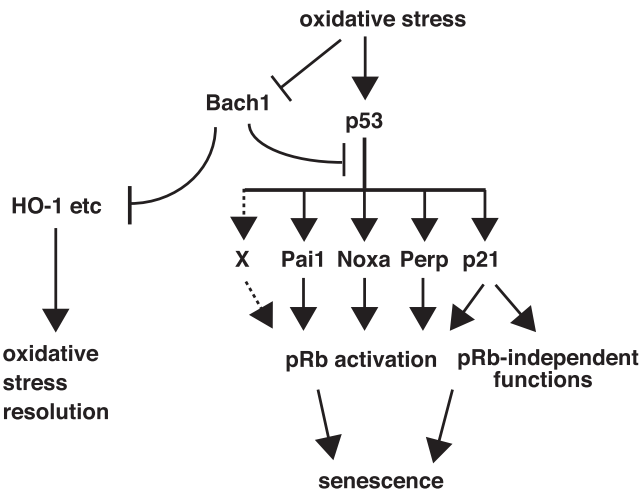

FIG. 7. A model of the gene network for cellular senescence. p53 target genes regulate cellular senescence by funneling into pRb-dependent and -independent subpathways. p21 and pRb may constitute linear as well as parallel subpathways. X indicates putative missing gene for senescence, and its putative function is shown with *dashed lines*.

Therefore, it will be interesting to examine possible involvement of *BACH1* in human cancer.

Besides the p53-dependent pathway, Bach1 acts as a repressor of the oxidative-stress response through the MARE-dependent genes including HO-1 (18, 22, 27, 31, 39). Although the knockdown of HO-1 in *Bach1*-deficient MEFs did not result in the reentry to the cell cycle, the possibility cannot be ruled out that HO-1 may be involved in cellular senescence. HO-1 is induced in the process of premature senescence of human fibroblasts (30) and possesses the cytoprotective function to confer a stress-resistant phenotype. It is especially noticeable that *Bach1* deficiency contributes to the reduction of ROS levels with 20% oxygen conditions rather than its increase coincident with the induction of cellular senescence in MEFs (17). Therefore, when taken together with the present results, cellular senescence in *Bach1*-deficient cells results from higher responsibility of the p53 and pRb systems compared with wild-type cells but not from higher ROS levels. These results suggest that Bach1 plays an important role in maintaining cell homeostasis by balancing the metabolism of ROS and senescence with the distinct mechanisms (Fig. 7).

A pitfall of this study is the utilization of RNAi to assess functions of genes. Because RNAi is usually not complete, residual levels of mRNA may be sufficient to maintain cells in the senescent state. However, the observation that a transient reduction of several mRNAs simultaneously resulted in the bypassing of senescence is considered to be proof that their genetic interaction is critical in achieving senescence. The partial loss of function in the RNAi experiments may recapitulate pathologic situations in which relevant mutated genes often retain some activities. We hope that further studies on Bach1 will shed new light on the mechanisms of cellular senescence, including subsequent bypassing mechanisms toward carcinogenesis.

Acknowledgments

We thank Dr. Nobuyuki Tanaka, Nippon Medical School, for valuable advice and reagents, and Dr. Shigeru Taketani, Kyoto

Institute of Technology, for anti-HO-1 antibody. Interpretation of data has been enriched by discussion with Prof. Keiko Nakayama (Tohoku University) and the members of our laboratory, including Tsuyoshi Ikura, Akihiko Muto, and Yasutake Katoh. This work was supported by grants-in-aid and the Network Medicine Global-COE Program from the Ministry of Education, Culture, Sports, Science and Technology, Japan. Additional initiative supports were from the Uehara Foundation, the Takeda Foundation, and the Astellas Foundation for Research on Metabolic Disorders. This work was also supported by Biomedical Research Core, Tohoku University School of Medicine.

Author Disclosure Statement

The authors have no competing financial interest in relation to the work described.

References

1. Abbas T and Dutta A. p21 in cancer: intricate networks and multiple activities. *Nat Rev Cancer* 9: 400–414, 2009.
2. Artavanis-Tsakonas S, Rand MD, and Lake RJ. Notch signaling: cell fate control and signal integration in development. *Science* 284: 770–776, 1999.
3. Attardi LD, Reczek EE, Cosmas C, Demicco EG, McCurrach ME, Lowe SW, and Jacks T. PERP, an apoptosis-associated target of p53, is a novel member of the PMP-22/gas3 family. *Genes Dev* 14: 704–718, 2000.
4. Banin S, Moyal L, Shieh S, Taya Y, Anderson CW, Chessa L, Smorodinsky NI, Prives C, Reiss Y, Shiloh Y, and Ziv Y. Enhanced phosphorylation of p53 by ATM in response to DNA damage. *Science* 281: 1674–1677, 1998.
5. Bartkova J, Rezaei N, Liontos M, Karakaidos P, Kletsas D, Issaeva N, Vassiliou LV, Kolettas E, Niforou K, Zoumpourlis VC, Takaoka M, Nakagawa H, Tort F, Fugger K, Johansson F, Sehested M, Andersen CL, Dyrskjot L, Orntoft T, Lukas J, Kittas C, Helleday T, Halazonetis TD, Bartek J, and Gorgoulis VG. Oncogene-induced senescence is part of the tumorigenesis barrier imposed by DNA damage checkpoints. *Nature* 444: 633–637, 2006.
6. Basak S, Jacobs SB, Krieg AJ, Pathak N, Zeng Q, Kaldis P, Giaccia AJ, and Attardi LD. The metastasis-associated gene Prl-3 is a p53 target involved in cell-cycle regulation. *Mol Cell* 30: 303–314, 2008.
7. Beltrao P, Cagney G, and Krogan NJ. Quantitative genetic interactions reveal biological modularity. *Cell* 141: 739–745, 2010.
8. Ben-Porath I and Weinberg RA. The signals and pathways activating cellular senescence. *Int J Biochem Cell Biol* 37: 961–976, 2005.
9. Berube C, Boucher LM, Ma WA, Wakeham A, Salmena L, Hakem R, Yeh WC, Mak TW, and Benchimol S. Apoptosis caused by p53-induced protein with death domain (PIDD) depends on the death adapter protein RAIDD. *Proc Natl Acad Sci U S A* 102: 14314–14320, 2005.
10. Brigelius-Flohe R. Tissue-specific functions of individual glutathione peroxidases. *Free Radic Biol Med* 27: 951–965, 1999.
11. Brugarolas J, Bronson RT, and Jacks T. p21 is a critical CDK2 regulator essential for proliferation control in Rb-deficient cells. *J Cell Biol* 141: 503–514, 1998.
12. Campisi J. Cellular senescence as a tumor-suppressor mechanism. *Trends Cell Biol* 11: S27–S31, 2001.
13. Collado M, Gil J, Efeyan A, Guerra C, Schuhmacher AJ, Barradas M, Benguria A, Zaballos A, Flores JM, Barbacid M, Beach D, and Serrano M. Tumour biology: senescence in premalignant tumours. *Nature* 436: 642, 2005.
14. d'Adda di Fagagna F, Reaper PM, Clay-Farrace L, Fiegler H, Carr P, Von Zglinicki T, Saretzki G, Carter NP, and Jackson SP. A DNA damage checkpoint response in telomere-initiated senescence. *Nature* 426: 194–198, 2003.
15. Dimri GP, Lee X, Basile G, Acosta M, Scott G, Roskelley C, Medrano EE, Linskens M, Rubelj I, Pereira-Smith O, et al. A biomarker that identifies senescent human cells in culture and in aging skin in vivo. *Proc Natl Acad Sci U S A* 92: 9363–9367, 1995.
16. Dirac AM and Bernards R. Reversal of senescence in mouse fibroblasts through lentiviral suppression of p53. *J Biol Chem* 278: 11731–11734, 2003.
17. Dohi Y, Ikura T, Hoshikawa Y, Katoh Y, Ota K, Nakanome K, Muto A, Omura S, Ohta T, Ito A, Yoshida M, Noda T, and Igarashi K. Bach1 inhibits oxidative stress-induced cellular senescence by impeding p53 function on chromatin. *Nat Struct Mol Biol* 15: 1246–1254, 2008.
18. Duckers HJ, Boehm B, True AI, Yet SF, San H, Park JL, Clinton Webb R, Lee ME, Nabel GL, and Nabel EG. Heme oxygenase-1 protects against vascular constriction and proliferation. *Nat Med* 7: 693–698, 2001.
19. Harper JW, Adami GR, Wei N, Keyomarsi K, and Elledge SJ. The p21 Cdk-interacting protein Cip1 is a potent inhibitor of G1 cyclin-dependent kinases. *Cell* 75: 805–816, 1993.
20. Hayflick L. The limited in vitro lifetime of human diploid cell strains. *Exp Cell Res* 37: 614–636, 1965.
21. Hou R, Liu L, Anees S, Hiroyasu S, and Sibinga NE. The Fat1 cadherin integrates vascular smooth muscle cell growth and migration signals. *J Cell Biol* 173: 417–429, 2006.
22. Igarashi K and Sun J. The heme-Bach1 pathway in the regulation of oxidative stress response and erythroid differentiation. *Antioxid Redox Signal* 8: 107–118, 2006.
23. Jackson AL and Loeb IA. The contribution of endogenous sources of DNA damage to the multiple mutations in cancer. *Mutat Res* 477: 7–21, 2001.
24. Kortlever RM, Higgins PJ, and Bernards R. Plasminogen activator inhibitor-1 is a critical downstream target of p53 in the induction of replicative senescence. *Nat Cell Biol* 8: 877–884, 2006.
25. Krtolica A, Parrinello Lockett S, Desprez PY, and Campisi J. Senescent fibroblasts promote epithelial cell growth and tumorigenesis: a link between cancer and aging. *Proc Natl Acad Sci U S A* 98: 12072–12077, 2001.
26. Oda E, Ohki R, Murasawa H, Nemoto J, Shibue T, Yamashita T, Tokino T, Taniguchi T, and Tanaka N. Noxa, a BH3-only member of the Bcl-2 family and candidate mediator of p53-induced apoptosis. *Science* 288: 1053–1058, 2000.
27. Oyake T, Itoh K, Motohashi H, Hayashi N, Hoshino H, Nishizawa/ M, Yamamoto M, and Igarashi K. Bach proteins belong to a novel family of BTB-basic leucine zipper transcription factors that interact with MafK and regulate transcription through the NF-E2 site. *Mol Cell Biol* 16: 6083–6095, 1996.
28. Pantoja C and Serrano M. Murine fibroblasts lacking p21 undergo senescence and are resistant to transformation by oncogenic Ras. *Oncogene* 18: 4974–4982, 1999.
29. Parrinello S, Samper E, Krtolica A, Goldstein J, Melov S, and Campisi J. Oxygen sensitivity severely limits the replicative lifespan of murine fibroblasts. *Nat Cell Biol* 5: 741–747, 2003.
30. Pascal T, Debacq-Chainiaux F, Boilan E, Ninane N. Raes M, and Toussaint O. Heme oxygenase-1 and interleukin-11 are overexpressed in stress-induced premature senescence of

human WI-38 fibroblasts induced by *tert*-butylhydroperoxide and ethanol. *Biogerontology* 8: 409–422, 2007.
31. Peyton KJ, Reyna SV, Chapman GB, Ensenat D, Liu XM, Wang H, Schafer AI, and Durante W. Heme oxygenase-1-derived carbon monoxide is an autocrine inhibitor of vascular smooth muscle cell growth. *Blood* 99: 4443–4448, 2002.
32. Pomerantz J, Schreiber-Agus N, Liegeois NJ, Silverman A, Alland L, Chin L, Potes J, Chen K, Orlow I, Lee HW, Cordon-Cardo C, DePinho RA. The Ink4a tumor suppressor gene product, p19Arf, interacts with MDM2 and neutralizes MDM2's inhibition of p53. *Cell* 92: 713–723, 1998.
33. Redies C, Vanhalst K, and Roy F. delta-Protocadherins: unique structures and functions. *Cell Mol Life Sci* 62: 2840–2852, 2005.
34. Sablina AA, Budanov AV, Ilyinskaya GV, Agapova LS, Kravchenko JE, and Chumakov PM. The antioxidant function of the p53 tumor suppressor. *Nat Med* 11: 1306–1313, 2005.
35. Sage J, Miller AL, Perez-Mancera PA, Wysocki JM, and Jacks T. Acute mutation of retinoblastoma gene function is sufficient for cell cycle re-entry. *Nature* 424: 223–228, 2003.
36. Sage J, Mulligan GF, Attardi LD, Miller A, Chen S, Williams B, Theodorou E, and Jacks T. Targeted disruption of the three Rb-related genes leads to loss of G(1) control and immortalization. *Genes Dev* 14: 3037–3050, 2000.
37. Sionov RV and Haupt Y. The cellular response to p53: the decision between life and death. *Oncogene* 18: 6145–6157, 1999.
38. Siva K, Venu P, Mahadevan A, and Inamdar, MS. Human BCAS3 expression in embryonic stem cells and vascular precursors suggests a role in human embryogenesis and tumor angiogenesis. *PLoS ONE* 2: e1202, 2007.
39. Sun J, Hoshino H, Takaku K, Nakajima O, Muto A, Suzuki H, Tashiro S, Takahashi S, Shibahara S, Alam J, Taketo MM, Yamamoto M, and Igarashi K. Hemoprotein Bach1 regulates enhancer availability of heme oxygenase-1 gene. *EMBO J* 21: 5216–5224, 2002.
40. Weinberg RA. The retinoblastoma protein and cell cycle control. *Cell* 81: 323–330, 1995.

Address correspondence to:
Prof. Kazuhiko Igarashi
Seiryo-machi 2-1
Sendai 980-8575
Japan

E-mail: igarashi@med.tohoku.ac.jp

Date of first submission to ARS Central, August 11, 2010; date of final revised submission, November 22, 2010; date of acceptance, November 26, 2010.

Abbreviations Used

7-AAD = 7-amino-actinomycin D
ATM = ataxia-telangiectasia mutated
Bach1 = BTB and CNC homology-1
Bcas3 = breast carcinoma amplified sequence 3
BrdU = bromodeoxyuridine
CDK = cyclin-dependent kinase
Fat1 = FAT tumor suppressor homologue 1
Gpx1 = glutathione peroxidase 1
GSK-3β = glycogen synthase kinase-3β
HDAC1 = histone deacetylase-1
HO-1 = hemeoxygenase-1
Lrdd = leucine-rich and death domain containing
MARE = Maf-recognition element
MEF = mouse embryonic fibroblast
Pai1 = plasminogen activator inhibitor 1
Pcdh7 = protocadherin 7
PCNA = proliferation cell nuclear antigen
PCR = polymerase chain reaction
PI3K = phosphoinositide 3-kinase
PKB = protein kinase B
pRb = retinoblastoma protein
Prl-3 = phosphatase of regenerating liver-3
RNAi = RNA interference
SA-β-gal = senescence associated-β-galactosidase

This article has been cited by:

1. A Nakanome, A Brydun, M Matsumoto, K Ota, R Funayama, K Nakayama, M Ono, K Shiga, T Kobayashi, K Igarashi. 2012. Bach1 is critical for the transformation of mouse embryonic fibroblasts by RasV12 and maintains ERK signaling. *Oncogene* . [CrossRef]
2. Hironari Nishizawa, Kazushige Ota, Yoshihiro Dohi, Tsuyoshi Ikura, Kazuhiko Igarashi. 2012. Bach1-mediated suppression of p53 is inhibited by p19ARF independently of MDM2. *Cancer Science* n/a-n/a. [CrossRef]